10IDM-0058

An Energy-Based Proper Model of an Automotive Fuel Delivery System

Greg Browne, Nicholas Krouglicof, and Geoff Rideout
Memorial University of Newfoundland

ABSTRACT

Mathematical modeling is widely used throughout any scientific industry when trying to predict the behavior of dynamic systems. Oftentimes it is desirable that these models be simple and efficient, while still delivering accurate data.

This paper builds and examines an energy-based (bond graph) model of an automotive fuel delivery system and suggests which elements are required to produce a Proper Model. The Model Order Reduction Algorithm (MORA) provides a mechanism to quantitatively rank each element in the model and determine its contribution to the system dynamics.

Utilizing this approach, a model is developed that retains 98% of the complete system energy from 12 of the most active of 25 elements. This model requires 46.6% less simulation time while continuing to provide an adequate prediction of the system response.

INTRODUCTION

Any design expert in the automotive industry will most likely use some form of mathematical modeling when analyzing a product or procedure. An accurate mathematical model is essential in determining the response of a system and reviewing its characteristics.

Bond graphs are an efficient way of describing multiport systems, in that the connections (bonds) between system elements have both an effort and a flow whose product is the power of the bond [1]. Moreover, bond graphs allow for the seamless interconnection of systems across energy domains (hydraulics, rotational mechanics, translational mechanics, electrodynamics, etc). Therefore, bond graphs are used as the preferred means of modeling presented in this paper.

The main subsystems of an automotive fuel delivery system are shown as a block diagram in Fig. 1.

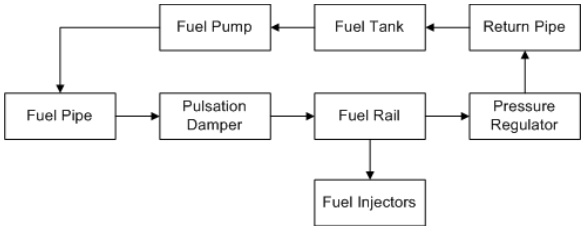

Fig. 1 Fuel Delivery System Block Diagram

MODEL CONSTRUCTION

To better understand the characteristics of the fuel delivery system, the subsystems can be generalized by their basic elements – shown as a schematic in Fig. 2.

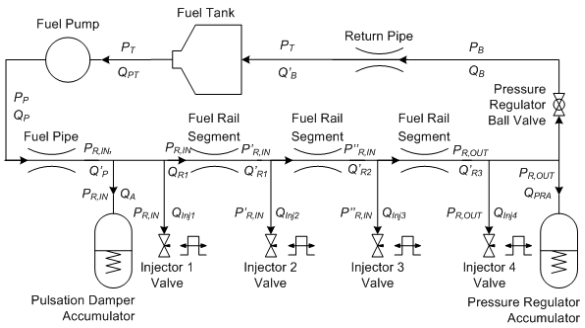

Fig. 2 Fuel Delivery System Schematic

The variables illustrated in Fig. 2 are used in the equations and derivations to follow.

Each subsystem can then be modeled individually based on the schematic. These subsystems are described in the following sections.

For quick reference, a table of bond graph elements can be found in Appendix A. For a more detailed description of bond graph formalism, the reader is referred to [1].

FUEL TANK

The simple function of the fuel tank is to store the fuel to be used by the system. Fuel is stored under slightly pressurized conditions, P_T, until it is drawn by the fuel pump. Unused fuel is returned to the tank via the return pipe.

The bond graph model for the fuel tank is shown in Fig. 3.

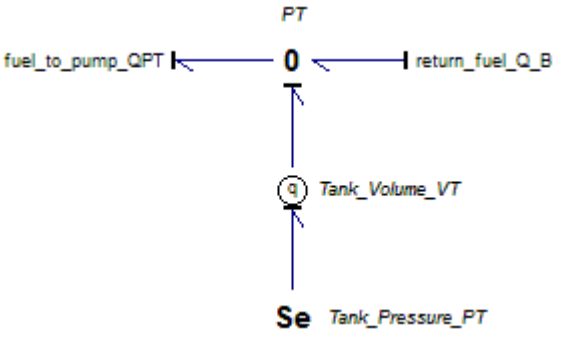

Fig. 3 Fuel Tank Submodel

The *q-sensor* is used to calculate the current tank volume by subtracting the amount of fuel used by the pump and re-accumulating the returned fuel to the initial volume, $V_T(0)$. This relationship is shown in Eq. (1).

$$V_T = V_T(0) + \int (Q'_B - Q_{PT})\, dt \qquad (1)$$

FUEL PUMP

The fuel pump (either in-tank or in-line) draws fuel from the fuel tank to be delivered to the system via the fuel pipe. Classically, a pump is modeled as an ideal flow source, Q_{PT}, with some internal leakage proportional to the pressure across the pump, P_P [2]. This relationship is shown in Eq. (2).

$$Q_P = Q_{PT} - C_P P_P \qquad (2)$$

Where, Q_P is the actual fuel flow delivered by the pump and C_P is the inherent leakage coefficient of the fuel pump (indicative of its volumetric efficiency).

This relationship is represented in bond graph form as illustrated in Fig. 4.

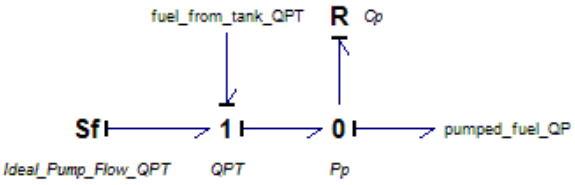

Fig. 4 Fuel Pump Submodel

FUEL PIPE

The fuel pipe delivers fuel from the fuel pump to the fuel rail. As fuel enters the fuel pipe, there will be an apparent loss in fluid flow due to its compressibility (bulk modulus, β), which is given by Eq. (3) [2].

$$\beta = -V_P(0)\frac{\partial P_P}{\partial V_P} \qquad (3)$$

Where, V_P is the volume of fuel in the fuel pipe.

The resulting fuel flow undergoes a pressure drop associated with the inertia, I, and resistance, R, of the fuel pipe, before being delivered to the fuel rail. The pressure drop due to pipe inertia is given by Eq. (4).

$$\Delta P = I\dot{Q} = \frac{\rho l}{A}\dot{Q} = \frac{4\rho l}{\pi D^2}\dot{Q} \qquad (4)$$

Where, ρ is the density of gasoline, l and D are the length and diameter of the fuel pipe, respectively.

The pressure drop due to the resistance of a pipe is non-linear, given by Eq. (5).

$$\Delta P = RQ^2 \qquad (5)$$

Furthermore, the resistance of a pipe varies based on the nature of the fluid flow that passes through it (determined by its Reynolds Number,

Re). This piece-wise relationship is given by Eq. (6).

$$R = \begin{cases} \frac{32\nu l\rho}{AD^2}, & Re \le Re_L \\ \left[\frac{64}{Re_L} + \left(\frac{0.3164}{Re_T^{0.25}} - \frac{64}{Re_L}\right)\left(\frac{Re - Re_L}{Re_T - Re_L}\right)\right]\frac{\rho l A^2}{2D}, & Re_L < Re < Re_T \\ \left(\frac{0.3164}{Re^{0.25}}\right)\frac{\rho l A^2}{2D}, & Re \ge Re_T \end{cases} \quad (6)$$

Where, ν is the viscosity of gasoline, A is the cross-sectional area of the fuel pipe, Re_L is the maximum Reynolds number for laminar fluid flow, and Re_T is the minimum Reynolds number for turbulent flow. The first part of the expression is the relationship for pipe flow with laminar flow, the last part is for turbulent flow [2], and the middle part is a linear interpolation function [3].

The Reynolds Number is calculated using Eq. (7).

$$Re = \frac{QD}{\nu A} \quad (7)$$

By combining Eq. (3)-(7), a relationship can be derived for output pressure, P_{out}, given by Eq. (8).

$$P_{out} = \frac{\beta}{V_P(0)}\int Q\,dt - \frac{4\rho l}{\pi D^2}\dot{Q} - RQ^2 \quad (8)$$

This relationship is represented in bond graph form as illustrated in Fig. 5.

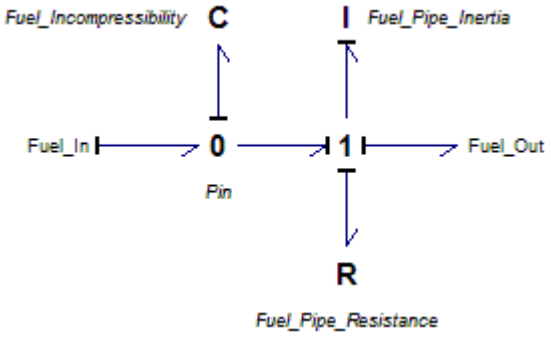

Fig. 5 Fuel Pipe Submodel

PULSATION DAMPER

The pulsation damper acts as an accumulator to smooth out the small drops in pressure created by the injectors during their firing sequence [4]. However, not all vehicles utilize a pulsation damper and instead rely on the fuel pressure regulator to account for any fluctuations in pressure as best it can.

A bolt is attached to a diaphragm that moves with changes in fuel pressure, $P_{R,in}$. This relationship is shown as Eq. (9).

$$P_{R,in} - P_{atm} = \frac{k_A}{A_A}\int Q_A\,dt \quad (9)$$

Where, P_{atm} is atmospheric pressure (101.325 kPa), k_A is the stiffness of the bolt/diaphragm assembly (the inverse of the compliance, C_A), A_A is the cross-sectional area of the pulsation damper, and Q_A is the fuel flow into the pulsation damper.

This relationship is represented in bond graph form as illustrated in Fig. 6.

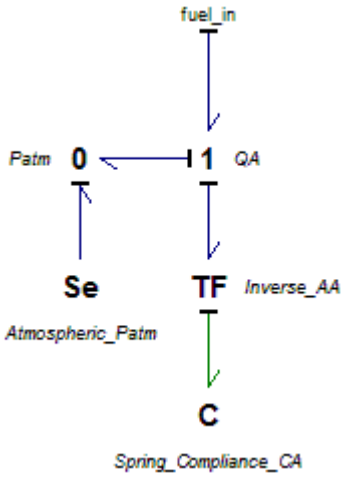

Fig. 6 Pulsation Damper Submodel

FUEL RAIL

The fuel rail is a pipe that delivers fuel to each of the fuel injectors (Q_{inj1} through Q_{inj4}). Unused fuel is returned to the fuel tank via the return pipe.

The piping between each injector will have restrictive effects similar to that discussed in the *Fuel Pipe* section – a change in fluid flow due to its compressibility (bulk modulus) and a pressure drop due to the inertia and resistance of the pipe segment.

The bond graph for the fuel rail is given in Fig. 7.

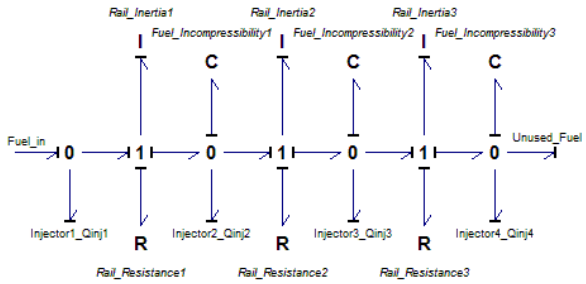

Fig. 7 Fuel Rail Submodel

FUEL INJECTORS

The fuel injectors take fuel from the fuel rail, atomize it, and spray it directly into the intake manifold of their respective cylinder.

A fuel injector consists of a solenoid-actuated pintle or needle valve [5] that is controlled by the vehicle ECU (Electronic Control Unit). The injected fuel flow, Q_{inj}, from the injector is given by Eq. (10).

$$Q_{inj} = \begin{cases} C_d A_V \sqrt{\frac{2}{\rho}(P_R - P_{man})}, & ON \\ 0, & OFF \end{cases} \quad (10)$$

Where, C_d is the internal discharge coefficient of the injector valve, A_v is the cross-sectional area of the injector valve, P_R is the rail pressure at the given injector, and P_{man} is the manifold pressure (MAP).

The *ON* condition in Eq. (10) deals with the two main factors that control the fuel injection – timing and quantity.

Some vehicles utilize "simultaneous fuel injection" whereby, at a given series of crank angles, all fuel injectors fire at the same time and for the same duration. This is a less interesting injection pattern and, hence, will not be discussed.

The most common type of electronic fuel injection (EFI) is "sequential fuel injection" (SFI). This is a more robust scheme, illustrated by example in Fig. 8, whereby at four different crank angles a single injector fires. This allows the system to make adjustments to fuel metering more quickly [4].

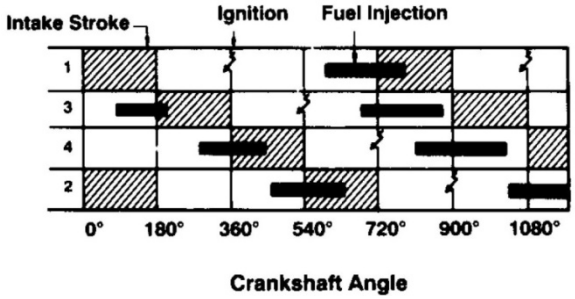

Fig. 8 Sequential Fuel Injection (SFI) Pattern [4]

The assumption is that each injector has a baseband crank angle, θ_B, at which, for all multiples of this angle, the given injector will fire. For simulation, these are assumed to be 180° for injector 1, 720° for injector 2, 360° for injector 3, and 540° for injector 4 (based loosely on Fig. 8).

It is also assumed that, at each particular triggering crank angle, the fuel injected will be half completed (i.e. the pulsed fuel will be centered about this trigger point).

The crank angle, θ_C, in degrees, can easily be derived from the engine RPM, as given by Eq. (11).

$$\theta_C = \frac{360}{2\pi}\int\left(\frac{2\pi}{60}\right) RPM\, dt = 6\int RPM\, dt \quad (11)$$

The quantity of fuel to be injected is converted to a pulse width, t_{ON}, during which the given injector is to fire. For a given load and negligible fuel trim, t_{ON} can be determined using Eq. (12).

$$t_{ON} = \frac{60(MAF)}{n_S R_{AF} \dot{m}_I (RPM)} \quad (12)$$

Where, MAF is the mass air flow rate (g/s), n_S is the number of strokes per revolution, R_{AF} is the air-fuel ratio, and $\dot{m}_I$ is the maximum fuel mass flow rate of the fuel injector (g/s).

However, the injection pattern is time-independent; therefore, it is more appropriate to express the fuel injection in terms of crank position. Therefore, the number of degrees the injector should fire per piston stroke, θ_{ON}, can be calculated using Eq. (13) (by multiplying the pulse width, given in Eq. (12), by the engine speed in deg/s).

$$\theta_{ON} = \frac{360(MAF)}{n_S R_{AF} \dot{m}_I} \quad (13)$$

For vehicles that do not have direct access to MAF (i.e. no MAF sensor is present), it is calculated by the ECU using Eq. (14) [6].

$$MAF = \frac{(MAP)(RPM)}{60 R_{air} T_{IA}} \left(\frac{V_{eng}}{2}\right) \quad (14)$$

Where, R_{air} is the specific gas constant for dry air, T_{IA} is the intake air temperature, and V_{eng} is the engine displacement (halved due to half the volume being swept during each revolution).

Considering Eq. (11) and Eq. (13), Eq. (10) can be re-written as Eq. (15).

$$Q_{inj} = \begin{cases} C_d A_V \sqrt{\frac{2}{\rho}(P_R - P_{man})}, & \left|\frac{\theta_{ON}}{2}\right| \leq (\theta_C \bmod 900) - \theta_B \\ 0, \ otherwise \end{cases} \quad (15)$$

A fuel injector is represented in bond graph form as illustrated in Fig. 9.

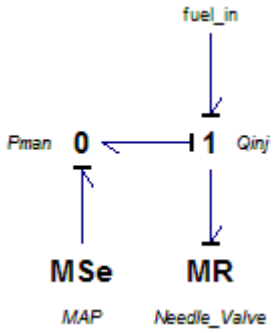

Fig. 9 Fuel Injector Submodel

FUEL PRESSURE REGULATOR

The fuel pressure regulator is a diaphragm-operated pressure relief valve that maintains a constant pressure differential across the fuel injectors [5]. This is accomplished by means of a ball valve, which is held in place by a preloaded spring against a diaphragm [4]. The regulated fuel rail pressure, $P_{R,out}$, is given by Eq. (16).

$$P_{R,out} = P_{R,in} - P_{man} - \frac{\rho}{2}\left(\frac{Q_{out}}{2\pi r_{out} x_R C_B}\right)^2 \quad (16)$$

Where, $P_{R,in}$ is the pressure of the fuel as it enters the pressure regulator, Q_{out} is the fuel out of the pressure regulator (given by Eq. (17)), r_{out} is the output radius of the pressure regulator, x_R is the displacement of the spring (the solution to the ODE given by Eq. (18)), and C_B is the discharge coefficient of the ball valve.

$$Q_{out} = Q_R - A_R \dot{x}_R \quad (17)$$

Where, Q_R is the fuel flow into the pressure regulator and A_R is the effective area of the pressure regulator that can be filled with fuel.

$$k_R x_R + B_R \dot{x}_R + M_R \ddot{x}_R = A_{RP}(P_{R,in} - P_{man}) - F_0 \quad (18)$$

Where, k_R is the pressure regulator spring stiffness, B_R is the viscous damping resulting from the volume of fuel present in the regulator, M_R is the mass of the regulator, A_{RP} is the effective area upon which pressure is exerted, and F_0 is the preload on the spring.

The bond graph representation of the fuel pressure regulator is given in Fig. 10.

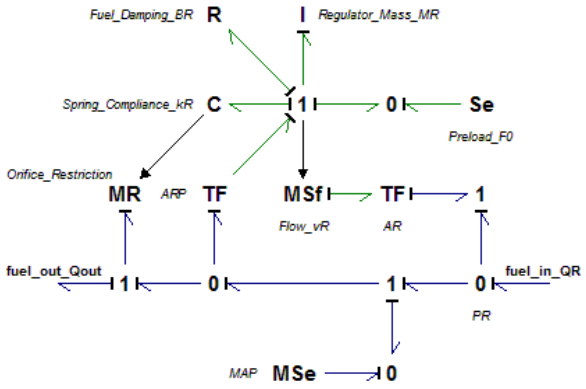

Fig. 10 Fuel Pressure Regulator Submodel

RETURN PIPE

The return pipe delivers the fuel from the pressure regulator back to the fuel tank to be recirculated by the system. The return pipe has the same submodel as previously discussed in the *Fuel Pipe* section.

SUBMODEL INTERCONNECTION

Due to the nature of bond graphs, the submodels can be easily interconnected to form the complete model previously outlined in the fuel delivery system schematic (Fig. 2). This complete model is shown in Fig. 11.

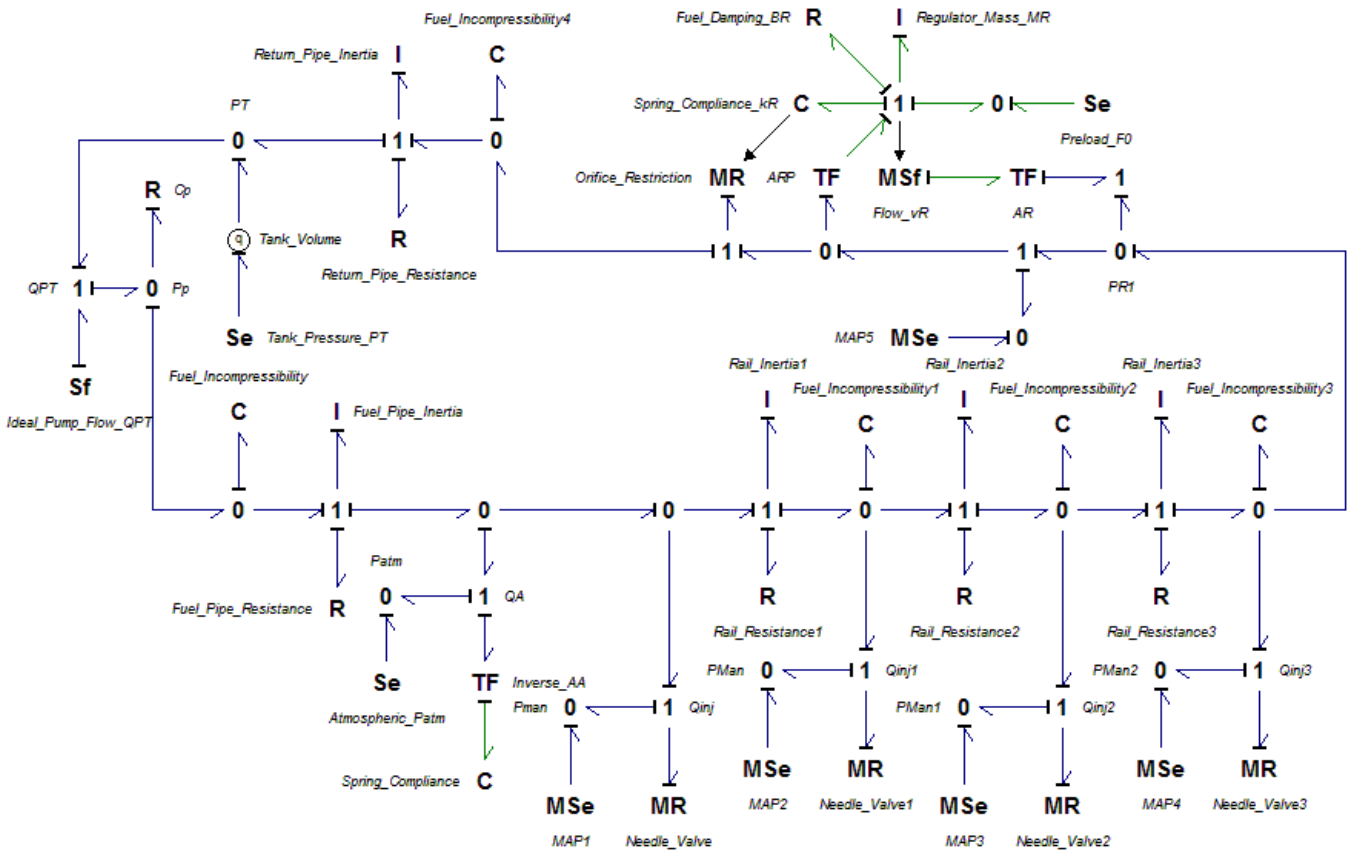

Fig. 11 Fuel Delivery System Complete Model

MODEL SIMULATION

Model construction and simulation is implemented in the software package *20-Sim*.

All system parameters used for simulation are given in Appendix B.

The required inputs to the model in order to produce a representative system response are manifold air pressure (MAP), engine RPM, and mass air flow (MAF). As previously discussed, MAF is either available directly or calculated using the previous two inputs in conjunction with intake air temperature (IAT).

In order to achieve the most accurate results, data was logged directly from a vehicle (2004 Chevrolet Optra) using a previously developed OBD-II hardware and software interface [7].

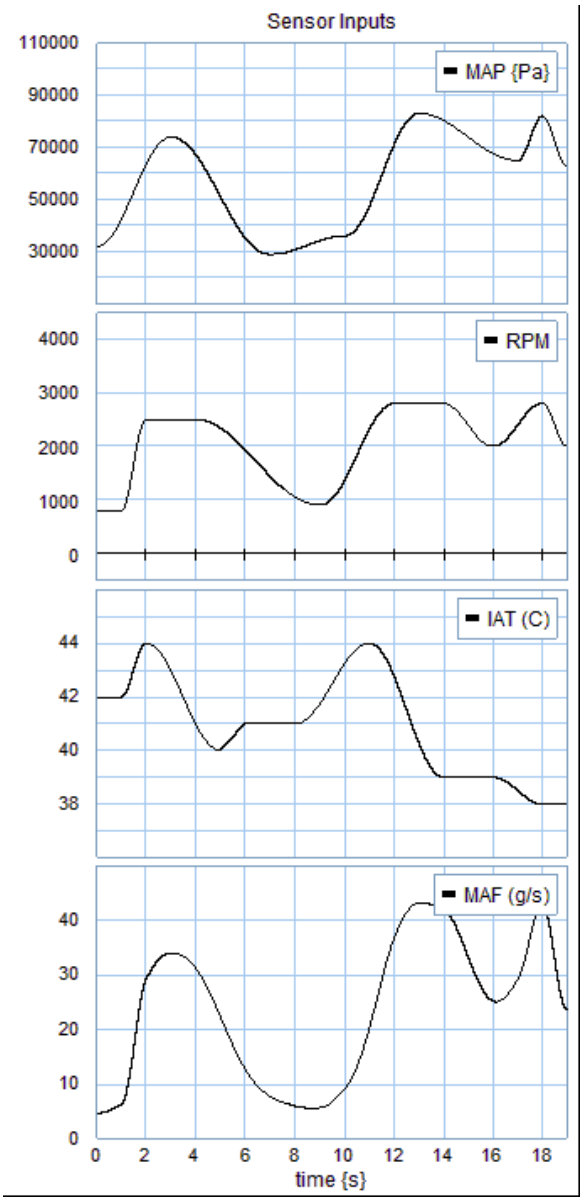

Fig. 12 Sensor Inputs

Logged sensor inputs were emulated as shown in Fig. 12. In this case, the Optra did not have a MAF sensor; therefore MAF was calculated as described in Eq (14).

The resulting pressure responses of interest are shown in Fig. 13.

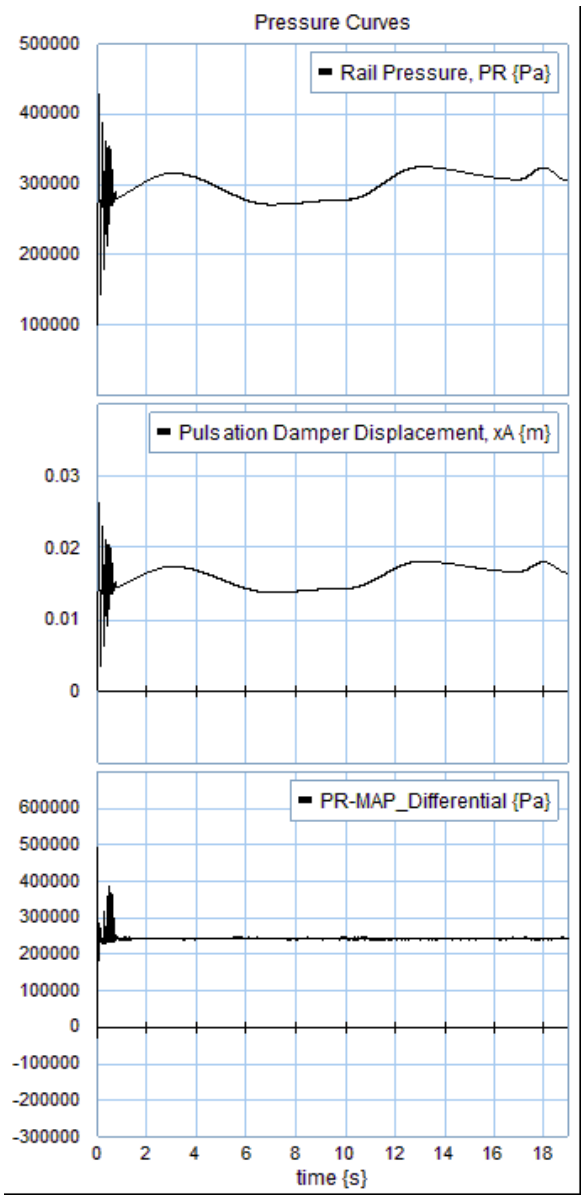

Fig. 13 Pressure Responses

One can see the pulsation damper accumulator displacement, x_A, acting in response to fluctuations in rail pressure, P_R.

The resulting flow responses of interest are shown in Fig. 14.

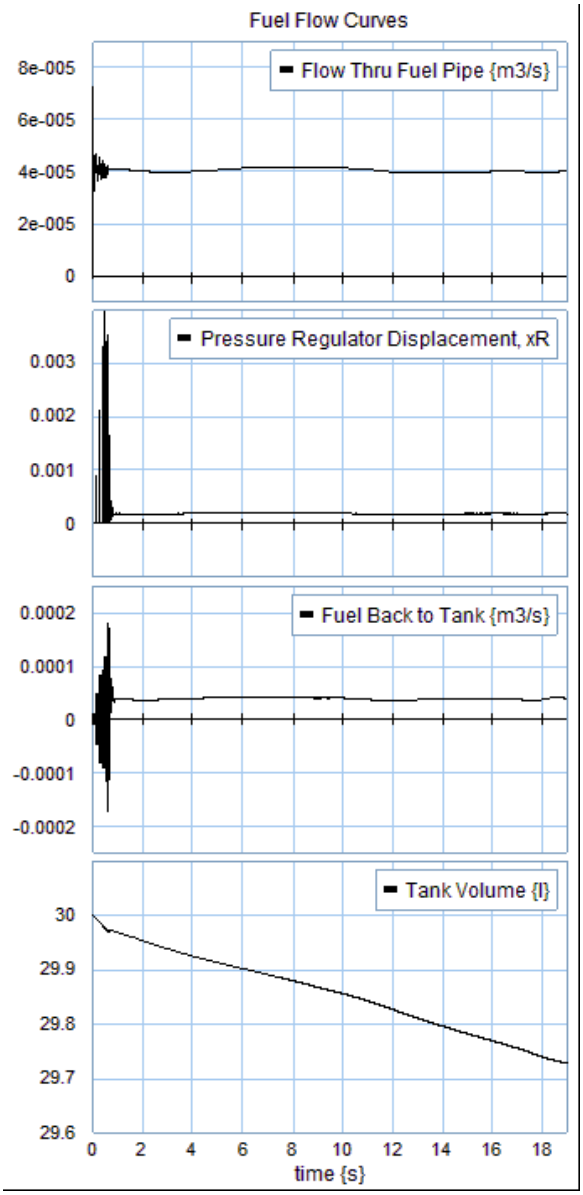

Fig. 14 Flow Responses

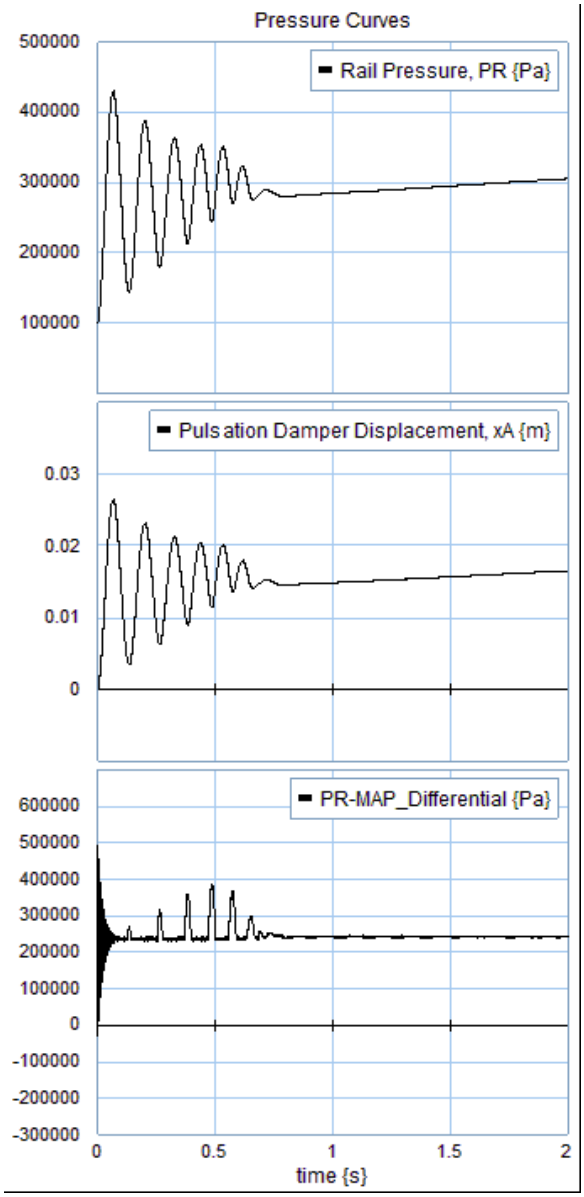

Fig. 15 Transient Pressure Responses

One can see the pressure regulator displacement, x_R, acting to maintain a constant differential between rail and manifold pressure (shown in Fig. 13). Also, it is shown that the fuel volume in the tank decreases, as expected, from an (arbitrary) initial volume of 30 L.

The initial transients are present for approximately the first second of simulation, and are better illustrated in Fig. 15 (transient pressure responses) and Fig. 16 (transient flow responses).

Any model used to describe a similar fuel injection system should aim to accurately reproduce the transients and steady-state responses, depending on the application.

Therefore, any elements that do not have an effect on these responses can effectively be removed without adversely changing the behavior of the system.

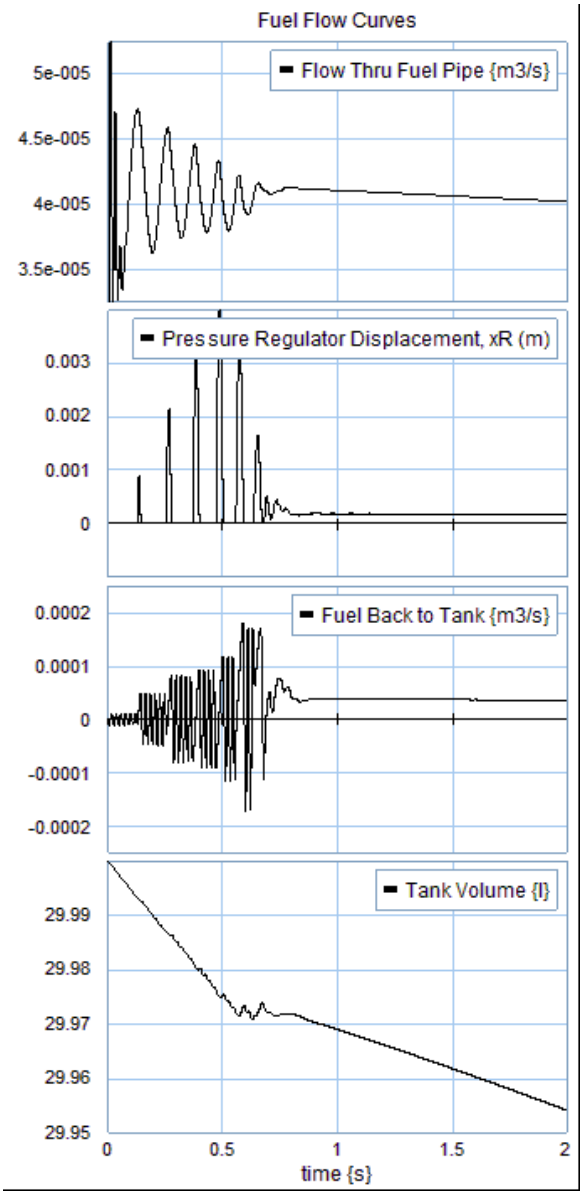

Fig. 16 Transient Flow Responses

MODEL REDUCTION

By utilizing a method that quantizes the contribution of each element, one can make an informed decision regarding which elements to retain and which to eliminate from a proper model. A proper model has minimal complexity, physically meaningful parameters, and accurately predicts dynamic system responses [8].

The Model Order Reduction Algorithm (MORA) uses activity, A_i, to quantize the contribution of a given element. Activity is "absolute energy" and, for a given element *i*, is calculated by Eq. (19) [8].

$$A_i = \int |P_i(t)|\, dt \qquad (19)$$

Where, P_i is the instantaneous power of element *i*.

Each element is assigned a non-dimensional activity index, AI_i, which is its fraction of the total system activity. For a given element *i* of *k* elements, its activity index is calculated using Eq (20) [8].

$$AI_i = \frac{A_i}{A_{Total}} = \frac{\int |P_i(t)|\, dt}{\sum_{i=1}^{k} \{\int |P_i(t)|\, dt\}} \qquad (20)$$

Activity indices are then sorted and elements eliminated from the lower end until the minimum number of elements required to satisfactorily reproduce the responses of the complete model is achieved.

ELEMENT ELIMINATION

Element activities and activity indices resulting from the simulations are given in Appendix C.

99% Model

By following the MORA algorithm to achieve a 99% model (a model that still retains at least 99% of the activity of the complete model), the following elements were eliminated:

- Needle Valves for Injectors 1 through 4
- Fuel Pipe Resistance
- Pressure Regulator Fuel Damping
- Return Pipe Resistance
- Fuel Pipe Fuel Incompressibility
- Fuel Pipe Inertia
- Fuel Rail Resistance 1 and 3

However, by strictly following the algorithm, one can see in the transient plots, Fig. 17 and Fig. 18 that the system responses acquire a high frequency infection and become less damped than the complete model.

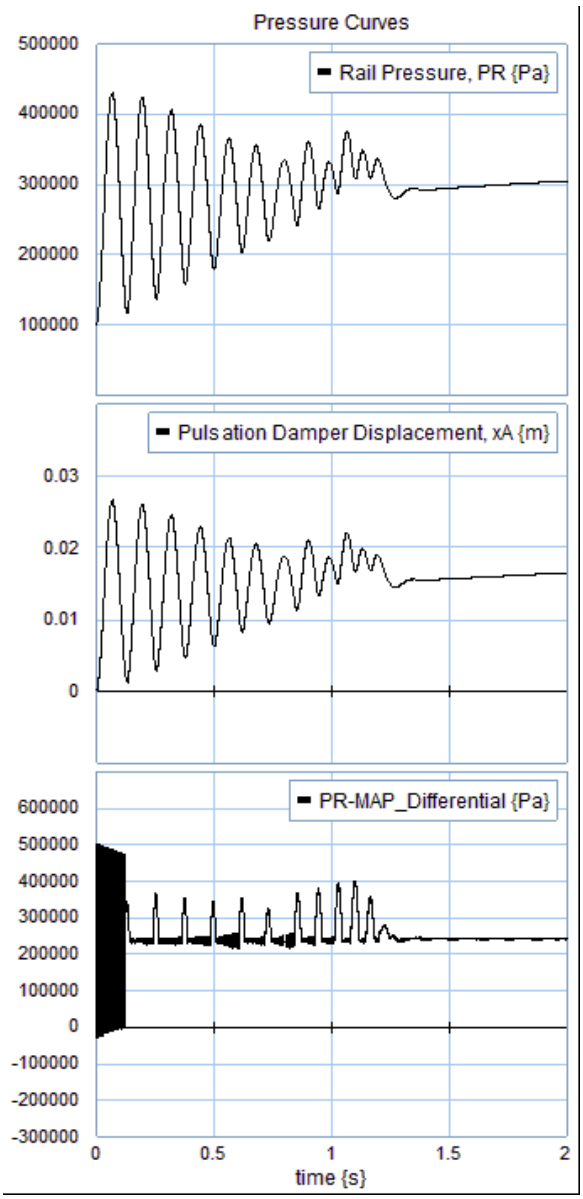

Fig. 17 99% Model Transient Pressure Responses

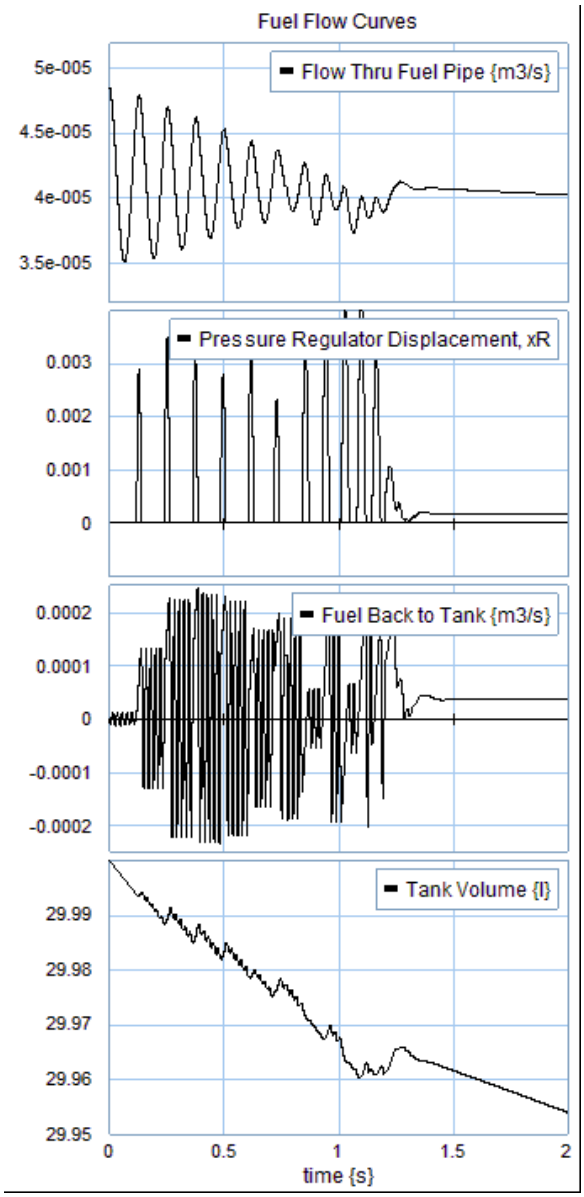

Fig. 18 99% Model Transient Flow Responses

High frequency infection is particularly noticeable in the pressure differential maintained by the pressure regulator (Fig. 17) as well as the fuel back to tank (Fig. 18).

The decrease in system damping is prevalent in each response shown.

However, if the fuel damping in the pressure regulator, B_R, is reinstated, the system responses can be returned to an adequate representation of the responses of the complete model.

This decision also has a physically intuitive basis – there must be some damping present in the mass-spring subsystem of the pressure regulator to prevent it from continuing to oscillate beyond a reasonable time constant.

98% Model

While maintaining B_R, the model can be further reduced to 98% by removing the following elements:

- Fuel Rail Resistance 2
- Pressure Regulator Mass, M_R

The transient responses of this 98% model are shown in Fig. 19 and Fig. 20.

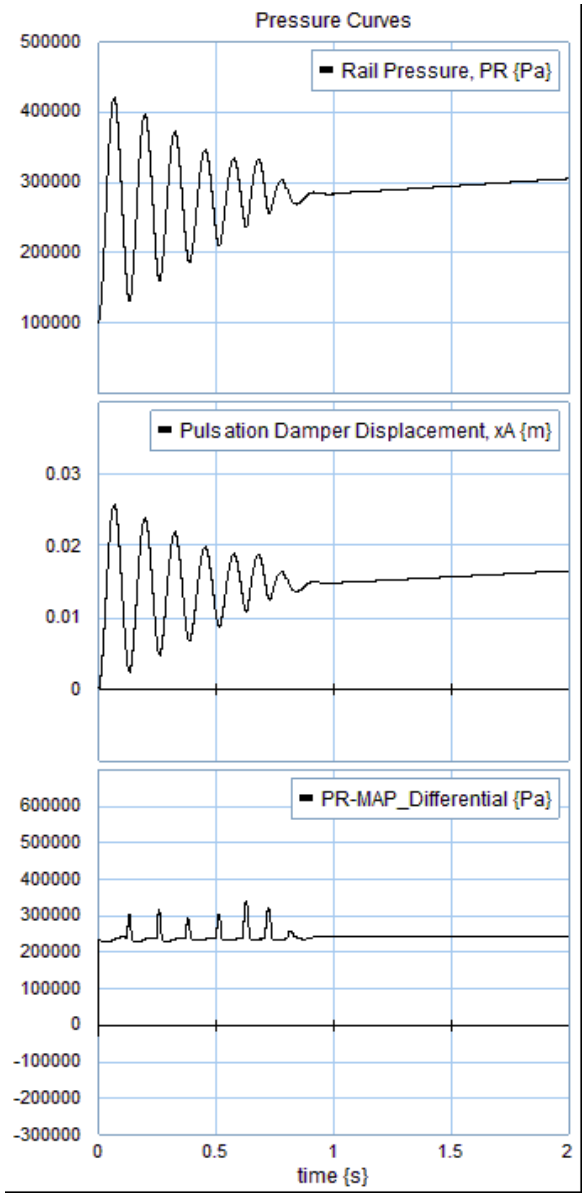

Fig. 19 98% Model Transient Pressure Responses

By comparing the transient pressure responses of the 98% model (Fig. 19) to that of the complete model (Fig. 15) one can see that the rail pressure, P_R, and the pulsation damper displacement x_A, are certainly replicated. The differential between P_R and MAP is fairly well replicated; however, the initial 4.7 kHz harmonic is missing from the 98% model. The suitability of this model will be based on the given application.

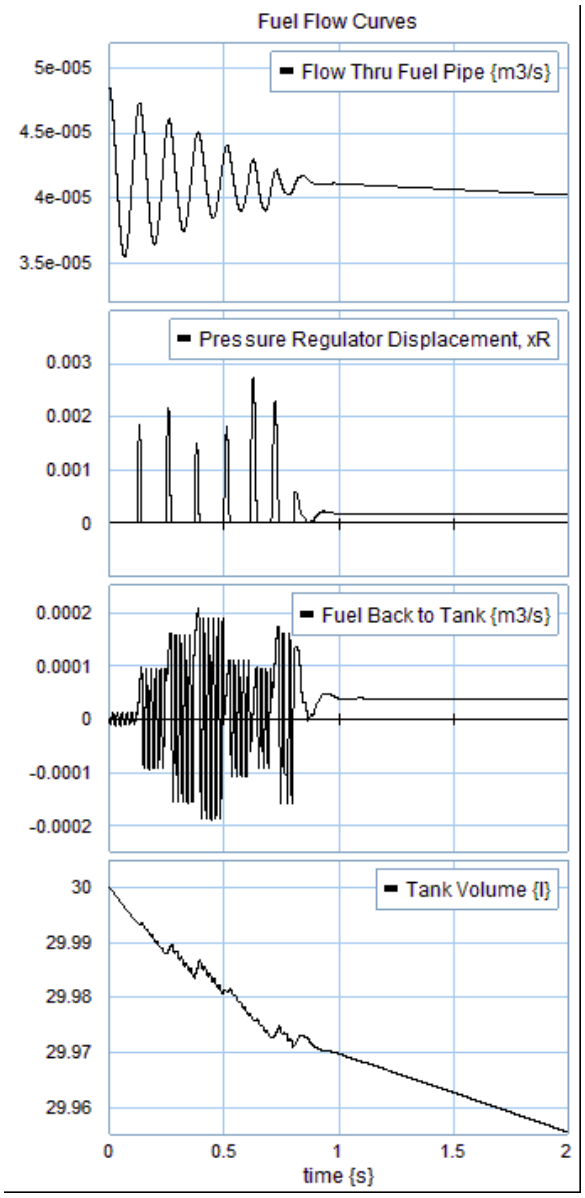

Fig. 20 98% Model Transient Flow Responses

By comparing the transient flow responses of the 98% model (Fig. 20) to that of the complete model (Fig. 16) one can again see that the 98% model is still a relatively accurate representation of the complete system. Yet again the suitability would have to be determined by the given application.

97% Model

To further reduce the model to 97% of the original system activity would require the elimination of the following element:

- Pressure Regulator Spring Stiffness, k_R

Eliminating k_R effectively adds infinite stiffness to an already massless diaphragm assembly in the pressure regulator. When considering the rail pressure differential transient, the system is now incapable of effectively responding with the proper overshoot, as shown in Fig. 21 (compared to Fig. 19).

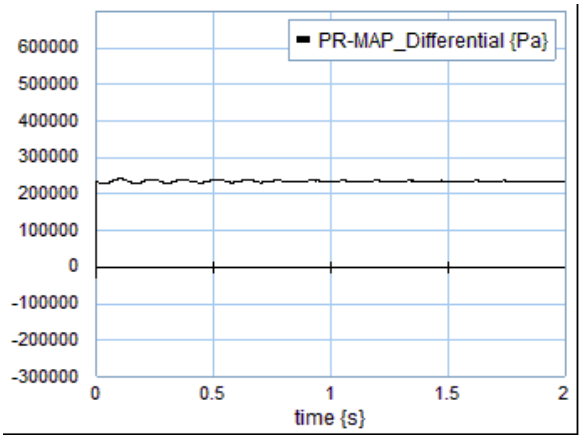

Fig. 21 97% Model Rail Pressure Differential Transient Response

Furthermore, the output fuel flow from the pressure regulator, given by Eq. (17), was originally constrained by Eq. (18). For the 97% model, Eq. (18) becomes Eq. (21).

$$B_R\dot{x}_R = A_{RP}\left(P_{R,in} - P_{man}\right) - F_0 \qquad (21)$$

This implies that any fluctuation in rail pressure, P_R, will cause an instantaneous change in the output flow from the pressure regulator. This is illustrated in Fig. 22.

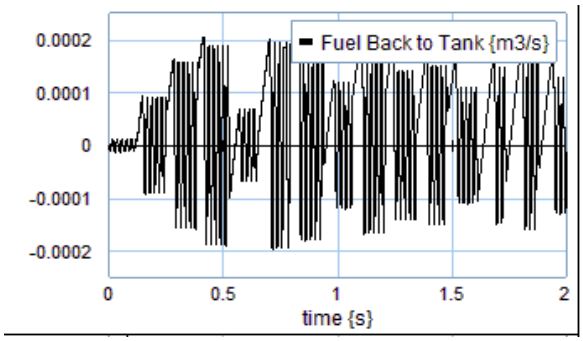

Fig. 22 97% Model Pressure Regulator Output Fuel Flow Transient Response

MODEL SELECTION

In many cases the 98% model will be a good choice for modeling a typical fuel injection system. The pressure and flow transients (Fig. 19 and Fig. 20) match reasonably well those of the complete model (Fig. 15 and Fig. 16).

The benefits to using the 98% model over the complete model include:

- Less complexity (less elements)
- Improved computational efficiency
  - 19.4% less computations required for simulation
  - 46.6% less computation/simulation time

The 98% model is shown in Fig. 23.

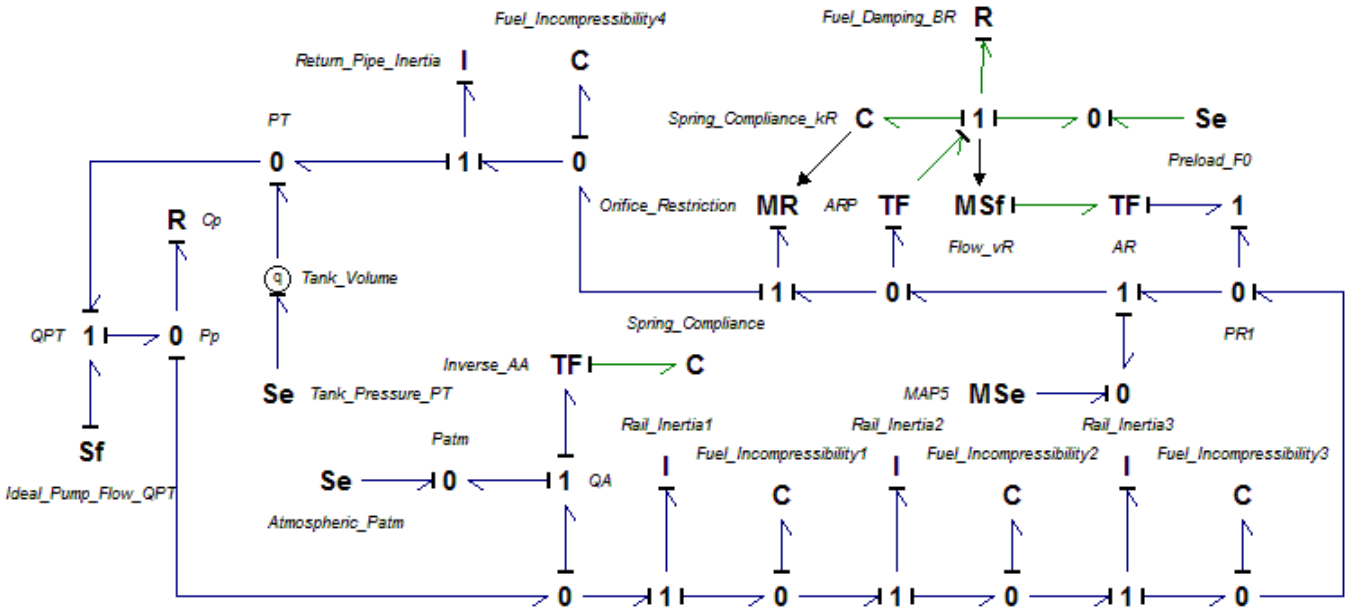

Fig. 23 98% Model

CONCLUSION

The reduced model presented in this paper was intended to provide an accurate representation of the complete system in terms of both transient and steady state responses.

However, the best selection of model to use will be based on the intended application for which it is to be applied. For example, if the intention is to study, in detail, the transient response, perhaps the complete model would be necessary in order to maintain the initial 4.7 kHz harmonic that was lost in the reduction process. Alternatively, if the study is focused on the steady state response of the system, the model could most likely undergo even further reduction than that presented in this paper.

Beyond the consideration of model activity, other elements may be retained if they are of particular interest. For example, the fuel injector needle valves could be retained if the fuel injection pattern was part of the intended study.

Regardless, this paper outlines the means by which one can reduce the complexity of a fuel delivery model, while still retaining the desired characteristics. Beyond reducing the computational complexity, the submodels of the system could also be imploded into iconic sections for easier analysis, as illustrated in Appendix D. A model with the proper degree of abstraction can be extremely useful as a design tool since it allows the engineer to focus on the elements of the system that have the greatest influence on performance.

REFERENCES

1. Karnopp, Dean C, Margolis, Donald L and Rosenberg, Ronald C. System Dynamics - Modeling and Simulation of Mechatronic Systems. 3rd. New York : Wiley-Interscience, 2000.
2. Merritt, Herbert E. Hydraulic Control Systems. New York: John Wiley & Sons, Inc., 1967.
3. Mathworks. Resistive Tube. MATLAB and Simulink for Technical Computing. [Online] February 9, 2009. [Cited: May 16, 2009.] http://www.mathworks.com/access/helpdesk/help/toolbox/physmod/simscape/ref/resistivetube.html.
4. Toyota Motor Sales, U.S.A., Inc. Fuel Delivery & Injection Control. [book auth.] U.S.A., Inc. Toyota Motor Sales. EFI Course Book. 2001, pp. 8,15.
5. Dynamic Modeling and Analysis of Automotive Multi-Port Electronic Fuel Delivery System. Yang, W C, et al. March 1991, Journal of Dynamic Systems, Measurement, and Control, Vol. 113, pp. 147-148.
6. On-Road Measurements of Emissions and Fuel Consumption of Gasoline Fuelled Light Duty Vehicles. Gonçalves, G A and Farias, T L. Lisbon: s.n., 2005. Clean Air 2005 - Eight International Conference on Technologies and Combustion for a Clean Environment. p. 9.
7. Browne, Greg. Design of Experiments to Determine Factors Contributing to Fuel Economy. Faculty of Engineering, Memorial University. St. John's: Unpublished, 2008.
8. Generating Proper Dynamic Models for Truck Mobility and Handling. Louca, Loucas S, et al. December 29, 2003, International Journal of Heavy Vehicle Systems, pp. 1,4.

CONTACT INFORMATION

g.browne@mun.ca

APPENDIX A: BOND GRAPH ELEMENTS

	SYMBOL	CONSTITUTIVE LAW (LINEAR)	CAUSALITY CONSTRAINTS
SOURCES			
Flow	Sf	f = f(t)	fixed flow out
Effort	Se	e = e(t)	fixed effort out
ENERGETIC ELEMENTS			
Inertia	I I	$f = \frac{1}{I}\int e\,dt$ $e = I\frac{df}{dt}$	preferred integral
Capacitor	C C	$e = \frac{1}{C}\int f\,dt$ $f = C\frac{de}{dt}$	preferred integral
Resistor	R R	$e = Rf$ $f = \frac{1}{R}e$	none
2-PORT ELEMENTS			
Transformer	TF, n	$e_2 = n\,e_1$ $f_1 = n\,f_2$	effort in-effort out or flow in-flow out
Modulated Transformer	MTF, n(θ)	$e_2 = n(\theta)\,e_1$ $f_1 = n(\theta)\,f_2$	
Gyrator	GY, n	$e_2 = n\,f_1$ $e_1 = n\,f_2$	flow in-flow out or effort in-effort out
Modulated Gyrator	MGY, n(θ)	$e_2 = n(\theta)\,f_1$ $e_1 = n(\theta)\,f_2$	
CONSTRAINT NODES			
1-junction	1, 3	$e_2 = e_1 - e_3$ $f_1 = f_2$ $f_3 = f_2$	one flow input
0-junction	0, 3	$f_2 = f_1 - f_3$ $e_1 = e_2$ $e_3 = e_2$	one effort input

APPENDIX B: SYSTEM PARAMETERS

Submodel	Parameter			
	Name	Value	Units	
Global	β	760	MPa	1
	ρ	737.22	kg/m^3	1
	ν	6.4×10^{-7}	m^2/s	1
	Re_L	2000		1
	Re_T	4000		1
Fuel Tank	P_T	1.1 * P_{atm}	Pa	2
Fuel Pump	Q_{PT}	5.28×10^{-5}	m^3/s	1
	C_P	4.11×10^{-11}	$m^3/s/Pa$	3
Fuel/Return Pipe	D	10	mm	2
	L	3.375	m	2
Pulsation Damper	A_A	0.001257	m^2	2
	k_A	15.63	kN/m	4
Fuel Rail	D	10	mm	2
	L	0.5	m	2
Fuel Injectors	C_dA_v	1.25×10^{-7}	m^2	4
Pressure Regulator	A_{RP}	0.00085	m^2	3
	A_R	0.000275	m^2	3
	B_R	2	Ns/m	2
	C_d	0.6		1
	r	3.1	mm	3
	F_0	200	N	2
	M_R	21.7	g	3
	k_R	31.5	kN/m	3

[1]Value typical to the industry

[2]Estimated value

[3]Value used from [5]

[4]Value determined through calculation

APPENDIX C: ELEMENT ACTIVITIES

Submodel	Element	Activity	Activity Index	Cumulative Activity	Comments
Pulsation Damper	Spring Compliance	38.239	19.433%	19.433%	Required elements to maintain 98% integrity.
Fuel Rail	Rail Inertia2	33.839	17.197%	36.630%	
Fuel Rail	Rail Inertia1	23.014	11.696%	48.325%	
Fuel Rail	Rail Inertia3	22.862	11.618%	59.943%	
Fuel Rail	Fuel Incompressibility1	14.981	7.613%	67.557%	
Fuel Rail	Fuel Incompressibility2	14.853	7.548%	75.105%	
Return Pipe	Return Pipe Inertia	14.153	7.192%	82.297%	
Return Pipe	Fuel Incompressibility	12.245	6.223%	88.520%	
Pressure Regulator	Orifice Restriction	8.085	4.109%	92.629%	
Fuel Pump	C_P	7.200	3.659%	96.288%	
Fuel Rail	Fuel Incompressibility3	2.017	1.025%	97.313%	
Pressure Regulator	Spring Compliance k_R	1.595	0.811%	98.124%	
Pressure Regulator	Regulator Mass M_R	1.388	0.705%	98.829%	Required to maint 99% integrity.
Fuel Rail	Rail Resistance2	0.366	0.186%	99.015%	
Fuel Rail	Rail Resistance3	0.364	0.185%	99.200%	
Fuel Rail	Rail Resistance1	0.364	0.185%	99.386%	
Fuel Pipe	Fuel Pipe Inertia	0.309	0.157%	99.543%	
Fuel Pipe	Fuel Incompressibility	0.301	0.153%	99.696%	
Return Pipe	Return Pipe Resistance	0.190	0.097%	99.793%	
Pressure Regulator	Fuel Damping B_R	0.134	0.068%	99.861%	Retained to prevent high freq.
Fuel Pipe	Fuel Pipe Resistance	0.092	0.047%	99.907%	
Inj1	Needle Valve	0.049	0.025%	99.932%	May be retained due to interest.
Inj4	Needle Valve	0.049	0.025%	99.957%	
Inj2	Needle Valve	0.044	0.022%	99.979%	
Inj3	Needle Valve	0.041	0.021%	100.000%	

TOTAL ACTIVITY:	196.774

APPENDIX D: ICONIC BOND GRAPH MODEL